Electronic Supplementary Material (ESI) for Analyst.

Supporting Information

Microraft array-based platform for sorting of viable microcolonies based on cell-lethal immunoassay of intracellular proteins in microcolony biopsies

Nicole M. Smiddy [a], Mathew DiSalvo [b], Jules D. Allbritton-King [b], Nancy L. Allbritton* [a, b, c]

[a] Department of Chemistry, University of North Carolina at Chapel Hill, Chapel Hill, NC, USA.

[b] Joint Department of Biomedical Engineering, University of North Carolina at Chapel Hill, Chapel Hill, NC, USA and North Carolina State University, Raleigh, NC, USA.

[c] Department of Bioengineering, University of Washington, Seattle, WA, USA.

*Corresponding Author

Nancy Allbritton. E-mail: nlallbr@uw.edu

Table of Contents

Experimental

Materials and reagents

Bovine serum albumin (BSA), and Triton X-100 were from Fisher Scientific (Hampton, NH). Fetal bovine serum (FBS) was from Atlanta Biologicals (Norcross, GA). Sodium chloride (NaCl) was acquired from VWR (Radnor, PA). 2,4-dinitrophenylated-BSA (DNP-BSA) was from Thermo Fisher. DNP-specific Immunoglobulin E (IgE), dimethyl sulfoxide (DMSO), sodium carbonate (Na_2CO_3), sodium bicarbonate ($NaHCO_3$), trisodium citrate ($Na_3C_6H_5O_7$), citric acid ($C_6H_8O_7$), potassium chloride (KCl), calcium chloride ($CaCl_2$), magnesium sulfate ($MgSO_4$), 4-(2-hydroxyethyl)-1-piperazineethanesulfonic acid (HEPES), glucose, 4-Methylumbelliferone, and 4-Methylumbelliferyl N-acetyl-β-D-glucosaminide were obtained from Sigma-Aldrich (St. Louis, MO). Phosphate buffered saline (PBS) was purchased from Corning (Corning, NY). CellTiter-Glo 2.0 Cell Viability Assay was obtained from Promega (Madison, WI).

Microarray Characterization

Micropillars on the negative molds used to make quad microraft arrays and microwell collection arrays were measured using a P-15 KLA-Tencor contact profilometer (Milpitas, CA). Quad microraft arrays and microwell collection arrays were imaged using an FEI Quanta 200 FEG Environmental SEM (Hillsboro, OR) after the array samples were coated with 5 nm Au using a Cressington 108 Auto Sputter Coater (Watford, UK).

Automated Microraft Biopsy

Biopsy automation was implemented as previously described.[1] Additionally, a maximum of 12 biopsy attempts per microraft was used to minimize experiment time and bypass colonies that were challenging to biopsy (which were returned to later for manual release). Each release attempt, the centroid-to-centroid displacement between the microraft and its microwell was calculated using automated image analysis. The displacement vector was used to translocate the microneedle below the microraft prior to needle actuation. To improve the robustness of the releases, the magnitude of the x and y components of the displacement vector was scaled by factors of 1×, 2.5×, or ½× (in this order, repeating cyclically for up to 12 releases) before using the vector to translocate the microneedle. The intent of modulating the needle position in this fashion was to improve the robustness of microraft ejection in scenarios where there is a small error in the detected vs. actual microraft centroid location. After the completion of biopsy, a 0.3 s pause was applied to permit the biopsied microraft to be collected prior to movement of the microscope stage to the next colony location.

Matching Biopsy Fragments to Mother Colonies

A MATLAB script was used to stitch whole-array images (64 images per full array) for each of the 3 array images (microwell collection array post-assay, microwell collection array post-collection, and microraft array post-biopsy). Image analysis was performed manually in Fiji software[4] to track microraft movement from images post-biopsy to post-collection to post-assay. First, the 3 stitched array images were registered. Then, overlay images were generated for post-biopsy/post-collection and post-collection/post-assay. Fragments detected post-assay were matched back to their locations post-collection. Then, fragments post-collection were matched

back to their initial location determined from the post-biopsy image. With the assayed fragments matched back to their original location on the microraft array, the quad site where the microraft originated from (still comprised of the original mother colony) was resampled for expansion and downstream assays.

Clonal Colony Detection

The graphical user interface (GUI) displays the bright field image of a single quad site at each day imaged and the user chooses the 'Yes' or 'No' (Fig. S2). The selection of 'Yes' meant that the colony started from a single cell and remained clonal (*i.e.* no apparent migration of cells from outside of the quad site). After selection, the GUI showed the next quad site to assess, and once all sites were evaluated a list of row and column locations for clonal quad colony sites was generated.

Proliferation Assay

To quantify cell proliferation, ATP concentration was measured as a surrogate for cell number using CellTiter Glo 2.0 Assay reagent as specified by the manufacturers' protocols. Briefly, cells were seeded into 96-well plates (N=5 wells per culture type). Each well started with 5,000 cells (100 μL/well). At the same time on each of the 3 days measured, the cells were incubated with 100 μL CellTiter-Glo reagent (which contained luciferine) and positioned on an orbital shaker for 2 min to lyse the cells. The luminescent product, oxyluciferin, was measured by an automatic plate reader (Spectra ax M5, Molecular Devices Corp.) at an integration time of 1000 ms. Luminescence was correlated to actual cell number using a standard curve made by counting cells and measuring the resulting signal (N=5 wells per cell number condition). Cell doubling

time (t_d) was quantified by fitting an exponential growth curve to a log (cell number) vs time plot and calculating the rate constant k via the equation $t_d = \ln(2)/k$.

β-hex Secretion Assay

The secretion of β-hexosaminidase (β-hex) was measured as previously described,[5, 6] with minor modifications. Specifically, cells of a 96-well plate coated with 2% (w/v) BSA were seeded with 100,000 cells per well. Cells were incubated with 0.1 μg/mL DNP-specific IgE for 20 h and then incubated with the antigen (0.1 μg/mL DNP-BSA) for 1 h. The supernatant was collected to measure β-hex secreted from the cells. To measure total β-hex, the cells were incubated in 1% Triton X-100 for 2 min and the cell lysate collected. The supernatant and cell lysate were incubated separately with an equal volume of 1 mM β-hex substrate in 0.1 M $C_6H_8O_7/Na_3C_6H_5O_7$ (pH 4.5) for 1 h and the reaction terminated with 0.1 M $Na_2CO_3/NaHCO_3$ (pH 10.0). Unless otherwise specified, solutions were prepared in Tyrode's buffer (119 mM NaCl, 5 mM KCl, 25 mM HEPES, 2 mM $CaCl_2$, 2 mM $MgSO_4$, 6 g/L glucose, 0.1% (w/v) BSA, pH 7.4) and incubation steps were performed at 37℃. The fluorescent product, 4-methylumbelliferone, was measured using a plate reader (Spectra ax M5, Molecular Devices Corp.) with a 355 nm excitation and 450 nm emission wavelength. Percent degranulation was calculated from the relative fluorescence units (RFU) measured using the equation: RFU of supernatant × 100/RFU of supernatant + cell lysate.

Figures

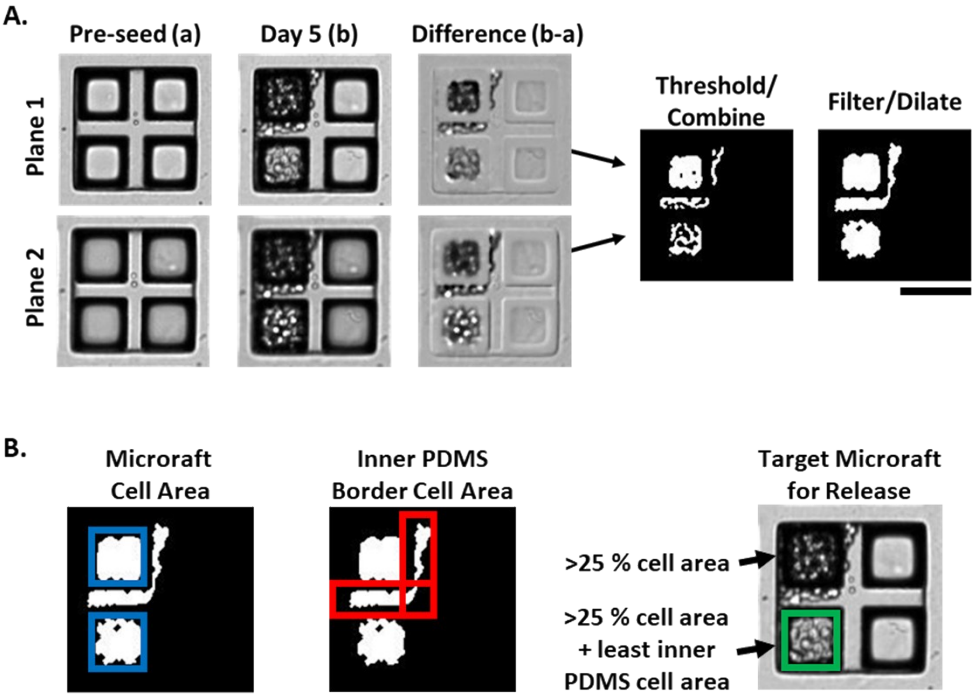

Fig. S1. Bright field detection of cells on quad microrafts. (A) Bright field microscopy images of quad microraft arrays were acquired at two different focal planes prior to cell seeding (a) and prior to biopsy on day 5 (b). Background subtracted images (b-a) from the two focal planes were used for cell segmentation by intensity thresholding and then the segmentation images generated (not shown). The segmented images from both focal planes were combined and morphological processing of images was applied to filter non-cellular objects and dilate pixels to close small gaps between objects in the image. The resulting cellular mask was used for measuring cellular area on microrafts and PDMS borders. Scale bar is 100 μm for all images. (B) Segmented images were used to measure cellular area on microrafts (blue outline) and adjacent inner PDMS borders (red outline). The microraft to target for colony biopsy (green outline) was defined as the microraft with ≥25 % cellular area and having the least cell connections outside the microraft border (*i.e.* lowest cellular area on adjacent inner PDMS borders) compared to other microrafts in the quad colony site with ≥25 % cellular area.

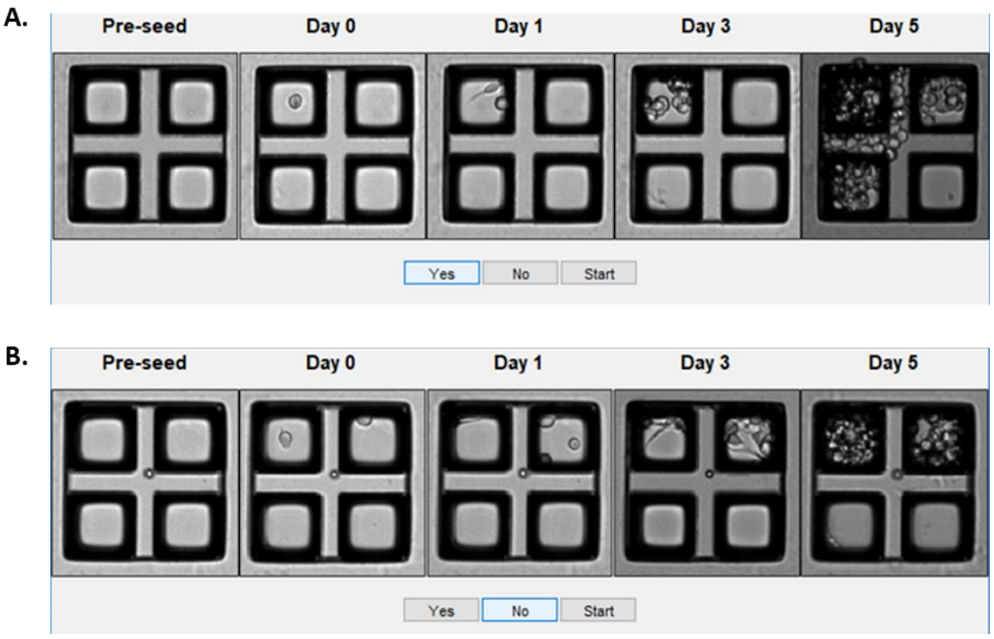

Fig. S2. Graphical user interface for clonal colony detection. (A) Target quad colony site that started with a single cell at day 0. (B) Non-target quad colony sites that started with two cells at day 0. Day 0 represents the image acquired immediately following cell seeding.

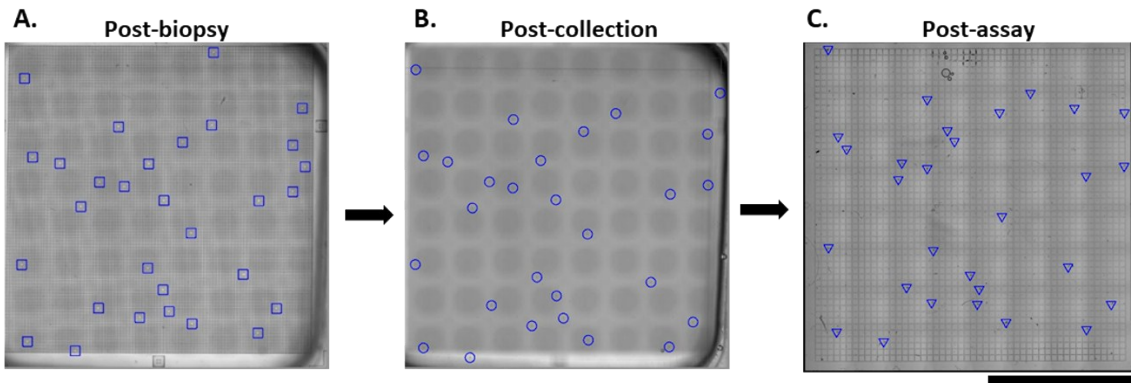

Fig. S3. Full array stitched images for tracking biopsied microrafts. (A) Full quad microraft array post-biopsy under EL light sheet illumination (N=64 images). Blue squares represent locations of biopsied microrafts. (B) Full microwell collection array (mated with microraft array) post-biopsy under EL light sheet illumination (N=64 images). Circles represent locations of collected microrafts. (C) Full collection array post-assay under bright field (unmated from microraft array and relocated to another chamber for assay) (N=64 images). Triangles represent microraft locations. In Post-biopsy and Post-collection images, the needle release device is positioned on the objective resulting in a pale circular shadow in the center each stitched image. The scale bar is 1 cm and is applied to all images.

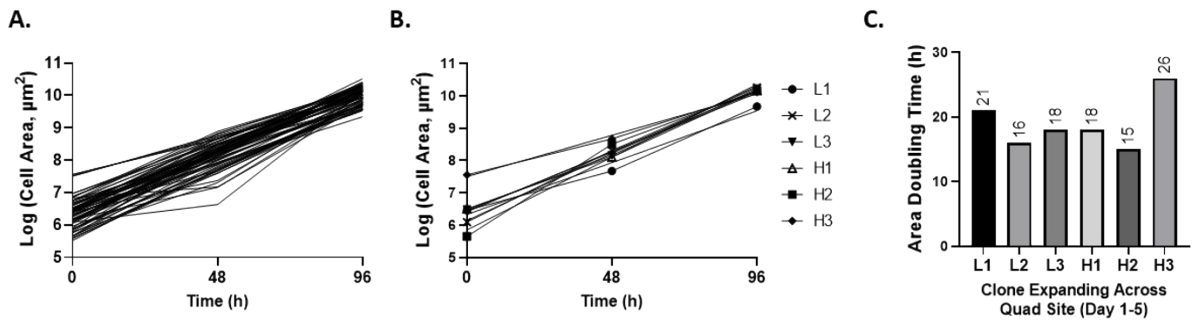

Fig. S4. RBL-2H3 microcolony doubling time on microrafts prior to biopsy. (A) For all 38 clonal colonies on quad microraft arrays identified prior to biopsy, a logarithmic plot showing the cellular area of each colony over 96 h (4 days) used to calculate doubling time (N=1 measurement per time point per colony). (B) Data extracted from the logarithmic plot in panel A for the 6 target clones identified based on pSTAT3/STAT3. (C) Cell area doubling time for the 6 target clones calculated at day 5 of growth on quad microrafts.

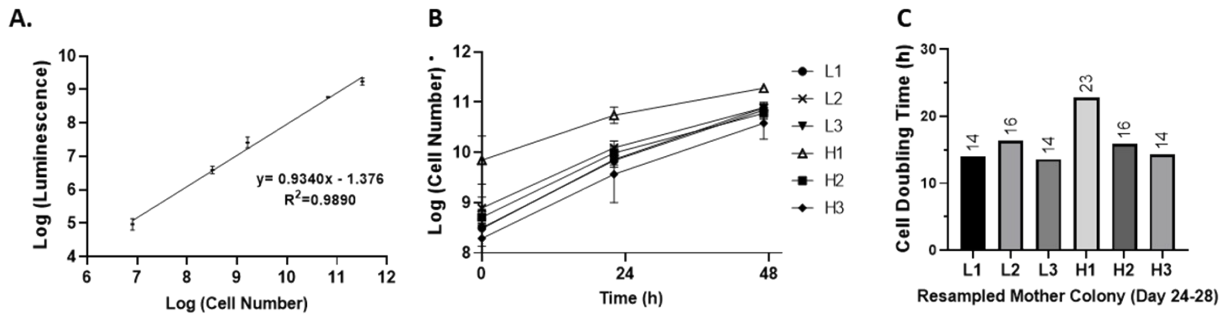

Fig. S5. Resampled mother RBL-2H3 colony doubling time in well plate. (A) For cells growing in a well plate, a logarithmic standard curve used to correlate luminescence signal from CellTiter Glo proliferation assay to cell number (N=3 wells per cell number). (B) For each of the 6 target clones, ~50,000 cells were seeded in a well plate and the cell number measured over 48 h (2 days) to calculate cell doubling time (N = 5 wells per clone). (C) Cell area doubling time for target clones calculated at days 24-28 of growth. All logarithmic plots are in natural log. Doubling time (t_d) was calculated from the rate constant k via the equation $t_d = \ln(2)/k$.

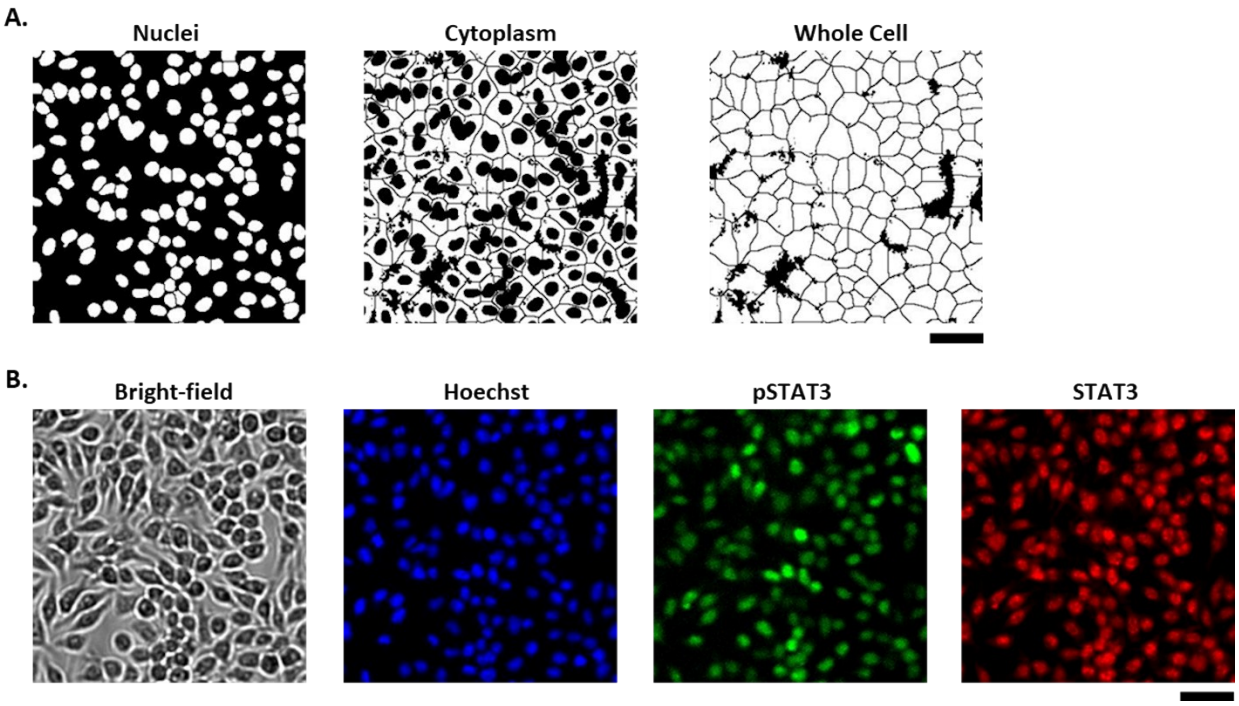

Fig. S6. Measuring immunofluorescence intensity from single cells. (A) Representative segmentation masks for cell nuclei, cytoplasm, and whole cell (nuclei and cytoplasm segmentations combined). Scale bar is 100 μm for all images. (B) Bright field and fluorescence microscopy images of RBL-2H3 cultures stained for Hoechst 33342, pSTAT3, and STAT3.

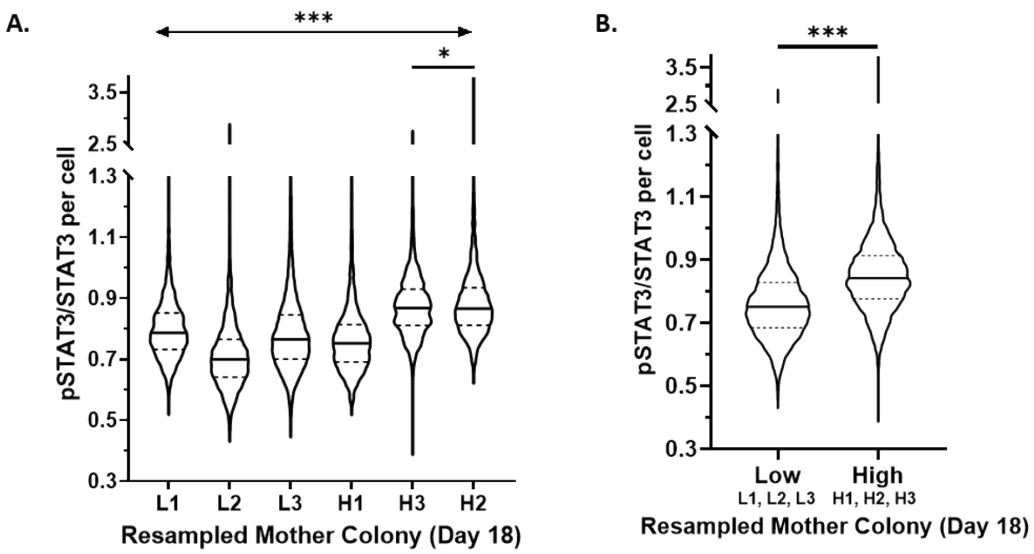

Fig. S7. Nuclear pSTAT3/STAT3 in resampled mother colony. (A) Distribution of pSTAT3/STAT3 per cell among the 6 resampled and expanded mother colonies at day 18 of culture (2,369 – 7,072 cells per clone). (B) The total distribution of pSTAT3/STAT3 per cell across the mother colonies at day 18 pooled according to the initial sort criteria: low (L1, L2, and L3) and high (H1, H2, and H3). For each violin plot, the solid horizontal line represents the median value, while dotted horizontal lines below and above the medium value represent the 25th and 75th percentile values, respectively. *p* values are represented as $p<0.05$ = *, $p<0.01$ = **, $p<0.001$ = ***.

References

(1) Freshney, R. I. *Cult. Anim. Cells* **2011**, *8*, 99–114.

(2) Wang, Y.; Phillips, C. N.; Herrera, G. S.; Sims, C. E.; Yeh, J. J.; Allbritton, N. L. *RSC Adv.* **2013**, *3* (24), 9264–9272.

(3) Disalvo, M.; Smiddy, N. M.; Allbritton, N. L. **2019**, *3*, 036106.

(4) Schindelin, J.; Arganda-Carreras, I.; Frise, E.; Kaynig, V.; Longair, M.; Pietzsch, T.; Preibisch, S.; Rueden, C.; Saalfeld, S.; Schmid, B.; Tinevez, J. Y.; White, D. J.; Hartenstein, V.; Eliceiri, K.; Tomancak, P.; Cardona, A. *Nat. Methods* **2012**, *9* (7), 676–682.

(5) Matsuda, H.; Tewtrakul, S.; Morikawa, T.; Nakamura, A.; Yoshikawa, M. *Bioorganic Med. Chem.* **2004**, *12* (22), 5891–5898.

(6) Matsubara, M.; Masaki, S.; Ohmori, K.; Karasawa, A.; Hasegawa, K. *Biochem. Pharmacol.* **2004**, *67* (7), 1315–1326.